AJNR

This information is current as of June 18, 2025.

High-field surface-coil MR imaging of localized anatomy.

J F Schenck, T H Foster, J L Henkes, W J Adams, C Hayes, H R Hart, Jr, W A Edelstein, P A Bottomley and F W Wehrli

High-Field Surface-Coil MR Imaging of Localized Anatomy

John F. Schenck,[1] Thomas H. Foster,[1] John L. Henkes,[1] William J. Adams,[1] Cecil Hayes,[2] Howard R. Hart, Jr.,[1] William A. Edelstein,[1] Paul A. Bottomley,[1] and Felix W. Wehrli[2]

For some time it has been recognized that surface-receiver-coil designs can enhance certain aspects of magnetic resonance (MR) signal detection [1]. During the last several years, surface coils have been the predominant means of recording the MR spectra of metabolites from animals and humans in vivo [2–4]. Efforts to produce surface-coil images at low magnetic field strengths have been undertaken as well [5, 6]. Recently, we exploited the properties of these coils to achieve enhanced sensitivity in MR imaging at 1.5 T [7]. Initial results demonstrate that significantly improved resolution of small anatomic structures is possible when surface coils are used as receiver elements in high-field MR imaging systems. We have been exploring this new technique as part of an ongoing effort to improve the diagnostic usefulness of MR in specific regions of the anatomy. Presented here are three series of images of the neck, the inner ear, and the lumbar spine obtained using the surface-coil method.

Materials and Methods

Our MR imaging system is built around an Oxford Instruments 1-m-bore 1.5 T superconducting magnet. The ^{1}H resonant frequency at this magnetic field strength is 63.9 MHz. All of the images in our study were recorded using separate radiofrequency (RF) transmitter and receiver coils. ^{1}H excitation was accomplished using a whole-body cylindrical coil with a diameter of about 51 cm. The images of the neck and of the inner ear were acquired using the same 13.5-cm-diam surface coil as the receiver element. In both cases, this flexible coil was shaped to conform closely to the region of anatomy under study. The lumbar spine was imaged with a slightly larger diameter (≈22 cm) surface-coil receiver to optimize sensitivity in the deeper pixels of interest. The RF fields of the transmitter and receiver coils were orthogonalized to minimize their mutual inductive coupling.

Throughout this investigation, the imaging slice thickness was 5 mm. There was no "dead space" between images. Images comprised 128 × 256 pixels, corresponding to a resolution in the plane of the image (except where noted in the figure legends) of about 1 × 0.5 mm. Pulse repetition times (TRs) and total scan time for each section are specified in the figure legends. A partial-saturation pulse sequence was used throughout, and images were recorded with our spin-warp spin-echo (SE) method [8]. Healthy volunteers served as the subjects for these studies. The offset slice capability of our imaging system was used so that the complete series of images in each anatomic region was acquired without repositioning the patient.

Results

A series of 12 transverse sections through the neck is shown in figure 1. The sequence proceeds from sections closest to the chest upward toward the head with a distance between centers of consecutive scans of 5 mm. Artifact caused by respiratory motion is apparent in figures 1A–1D. The detail of the arteries and veins of the neck is particularly encouraging. Good discrimination between thyroid and adjacent muscular (and possibly parathyroid) tissue is noted as well.

Figure 2 shows nine consecutive sagittal sections through the ear, external meatus, and inner ear; figure 3 is a coronal sequence in the same region. The sensitivity of the surface coil is well illustrated in figure 3A. Signal strength is excellent within the semicircular region that has a radius approximately equal to that of the surface coil and falls off rapidly for more remote pixels. Resolution of fine anatomic detail in the inner ear is afforded by the technique in the two imaging planes.

The sensitive region of a larger surface coil receiver is demonstrated in figure 4A. Figures 4B–4E show a series of consecutive sagittal sections through the lumbar spine. Pulse TRs, total scantimes, and resolution in the plane of the image are provided in the figure legends.

Discussion

The development of the surface-coil technique is an important aspect of advancing the capabilities of MR imaging and establishing MR's role in specific clinical applications. These experiments confirm our earlier findings that the use of modified surface-coil receivers in high-magnetic-field MR imaging systems generates sufficiently improved signal-to-noise (S/N) ratio to permit a significant reduction in the imaging voxel size. This reduction, achieved through the application of stronger imaging gradient fields, is responsible for the im-
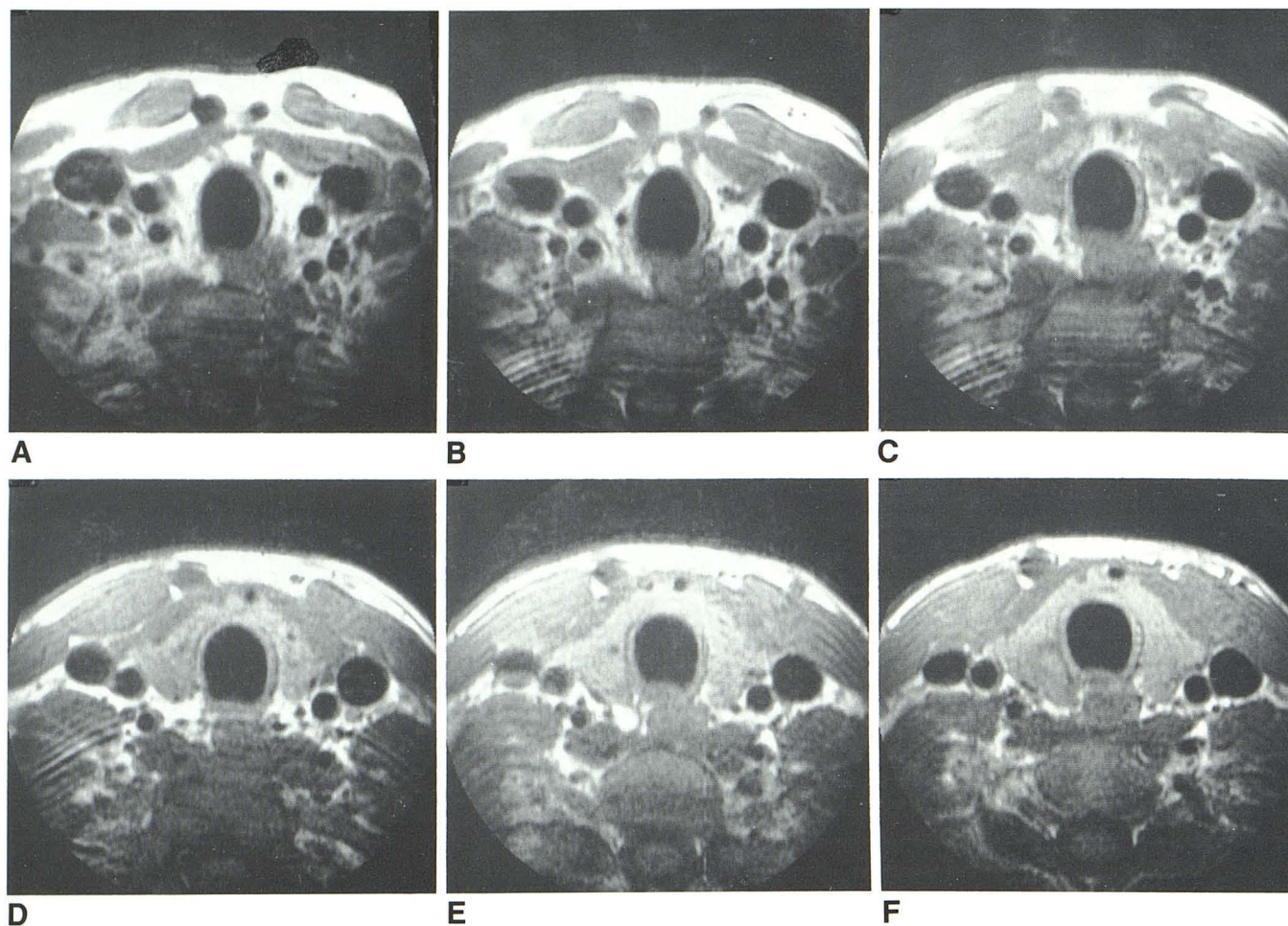
Fig. 1.—Axial sections through neck using 13.5-cm-diam flexible surface-coil receiver. Slice thicknesses and distances between centers of consecutive slices are all 5 mm. Image size is 128 × 256 pixels; pixel size is 1 × 0.5 mm. **A–C**, TR = 500 msec; **D–L**, TR = 300 msec. Scan times were 256 sec for **A–C** and 154 sec for **D–L**. (**A–F** are above; **G–L** are on facing page.)

proved resolution of anatomic detail observed in these images. The 1 × 0.5 × 5 mm picture-volume elements achieved here are smaller by a factor of two than those typically obtained in our imaging system when standard head-sized cylindrical RF coils are used as transmitter/receiver elements [10].

The ability to obtain high-resolution images of regions of anatomy not readily accessible to standard MR coils is an-

G   H   I

J   K   L
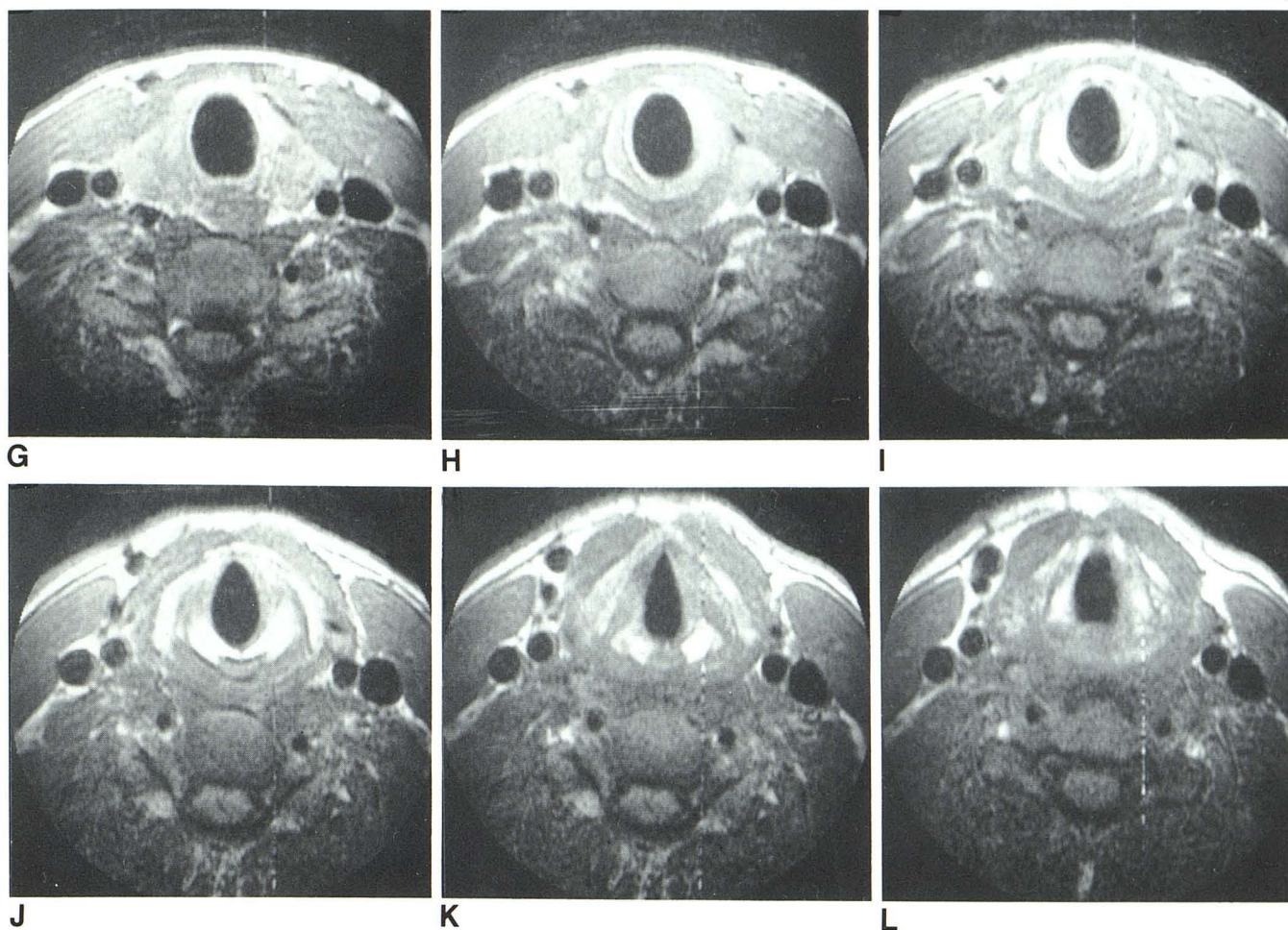
other advantage offered by the surface-coil technique. When, for example, the neck is imaged with an RF coil large enough to accept the whole body, the arrangement yields relatively poor coupling between ^{1}H nuclei in the neck and the coil and results in a suboptimal S/N ratio. The surface-coil receiver, on the other hand, may be fashioned to conform closely to the surface of the neck, thereby enhancing the magnetic flux linkage between the nuclear spins and the coil while at the
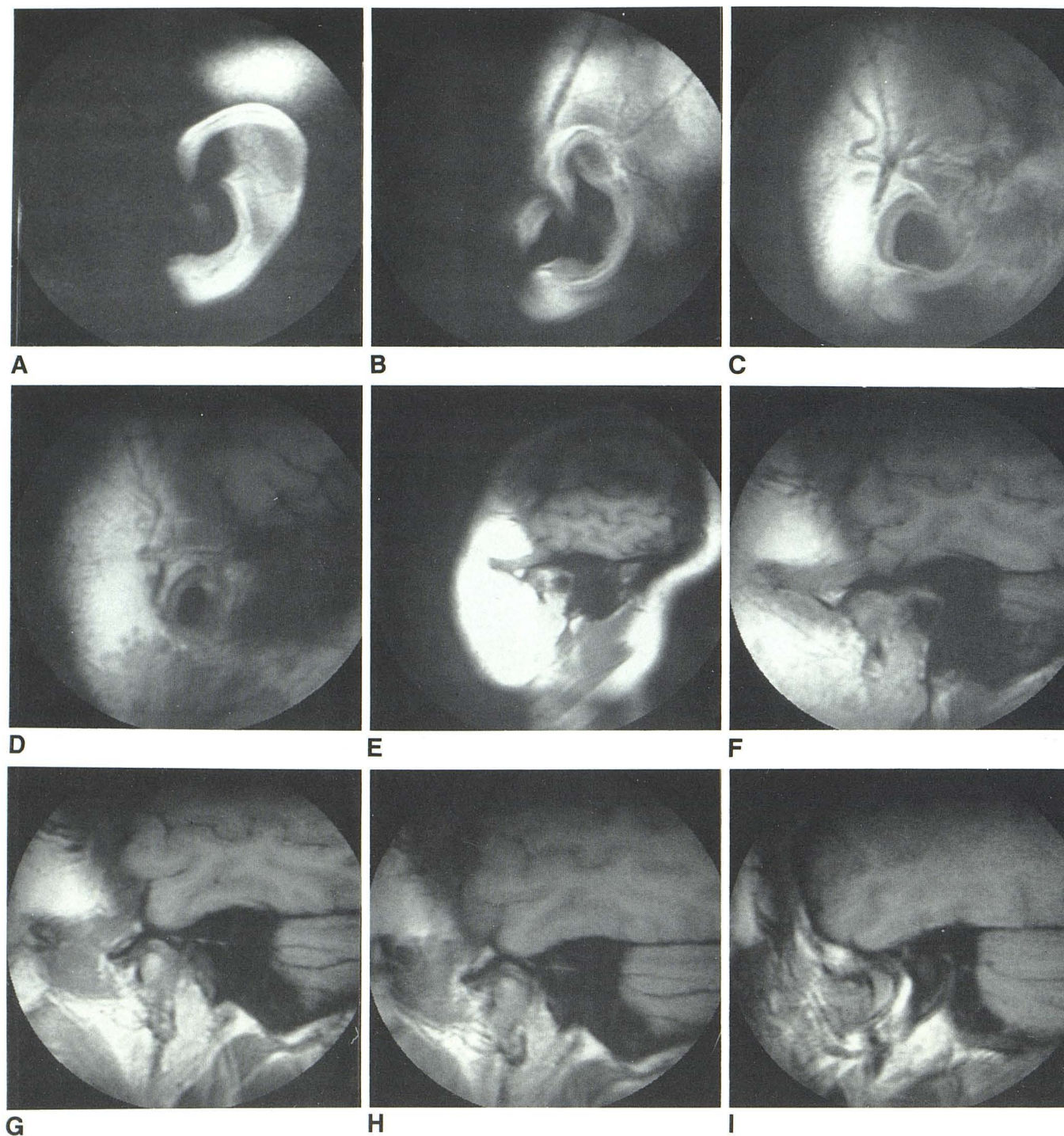
Fig. 2.—Parasagittal sections through ear and auditory canal. TR = 300 msec. Field of view in **E** is 250 × 250 mm, corresponding to resolution in plane of image of 2 × 1 mm; total scan time was 77 sec. Other images have 1 × 0.5 mm resolution and were recorded in 154 sec/slice. Distance between centers of consecutive sections is 5 mm in all but one instance: **F** and **G** are separated by only 2.5 mm. Slice thicknesses are 5 mm.

Fig. 3.—Coronal images through inner ear. Field of view in **A** is 250 × 250 mm, corresponding to resolution in plane of image of 2 × 1 mm; total scan time was 77 sec. Other images have 1 × 0.5 mm resolution and were recorded in 154 sec/slice. Distances between centers of consecutive slices are 2.5 mm in **B–D** and 5 mm between **A** and **B**. (**C** is reprinted from [9].)

A

B

C

D
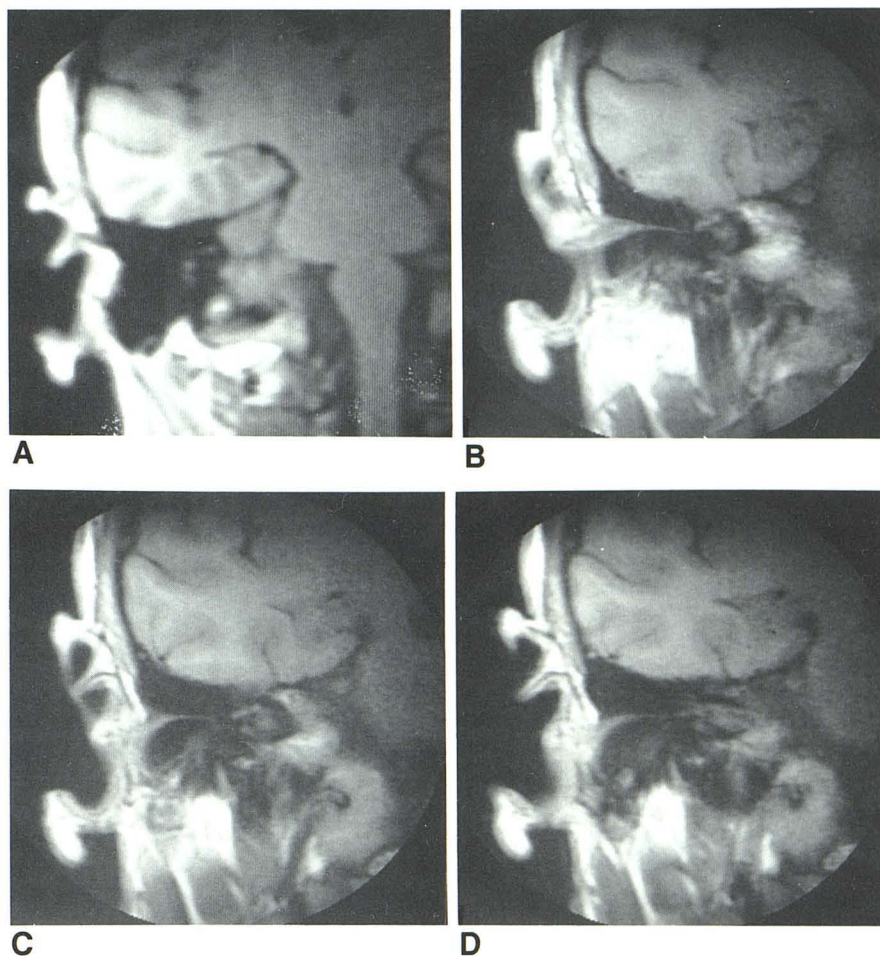
same time greatly reducing the received patient generated noise voltage.

The method we describe involves no modification to the MR imaging system other than the introduction of separate transmitter and receiver cells. This fact, together with the improvement in image content obtained, immediately raises the possibility of coupling the surface-coil technique with other emerging MR methods. Recently, for example, a chemical-shift imaging scheme was described and demonstrated whereby water (H_2O) or lipid ($-CH_2-$) protons may be imaged independently [11]. The ability to perform this type of imaging under the high-resolution conditions offered by surface coils may enhance MR's capability to diagnose atherosclerotic lesions of the carotid and vertebral arteries. Work will continue in an effort to further optimize surface-coil design for specific regions of the anatomy.

ACKNOWLEDGMENTS

REFERENCES

1. Zhernovoi AI, Latyshev GD. *Nuclear magnetic resonance in a flowing liquid.* New York: Plenum, **1965**:70
2. Ackerman JJH, Grove TH, Wong GG, Gadian DG, Radda GK. Mapping of metabolites in whole animals by ^{31}P using surface coils. *Nature* **1980**;283:167–170
3. Alger JR, Behar KL, Rothman DL, Shulman RG. Natural-abundance ^{13}C NMR measurement of hepatic glycogen in the living rabbit. *J Magnetic Resonance* **1984**;56:334–337
4. Bottomley PA, Hart HR, Edelstein WA, et al. NMR imaging/spectroscopy system to study both anatomy and metabolism. *Lancet* **1983**;2:273–274
5. Alfidi RJ, Haaga JR, El Yousef SJ, et al. Preliminary results in humans and animals with a superconducting whole-body, nuclear magnetic resonance scanner. *Radiology* **1982**;143:175–181
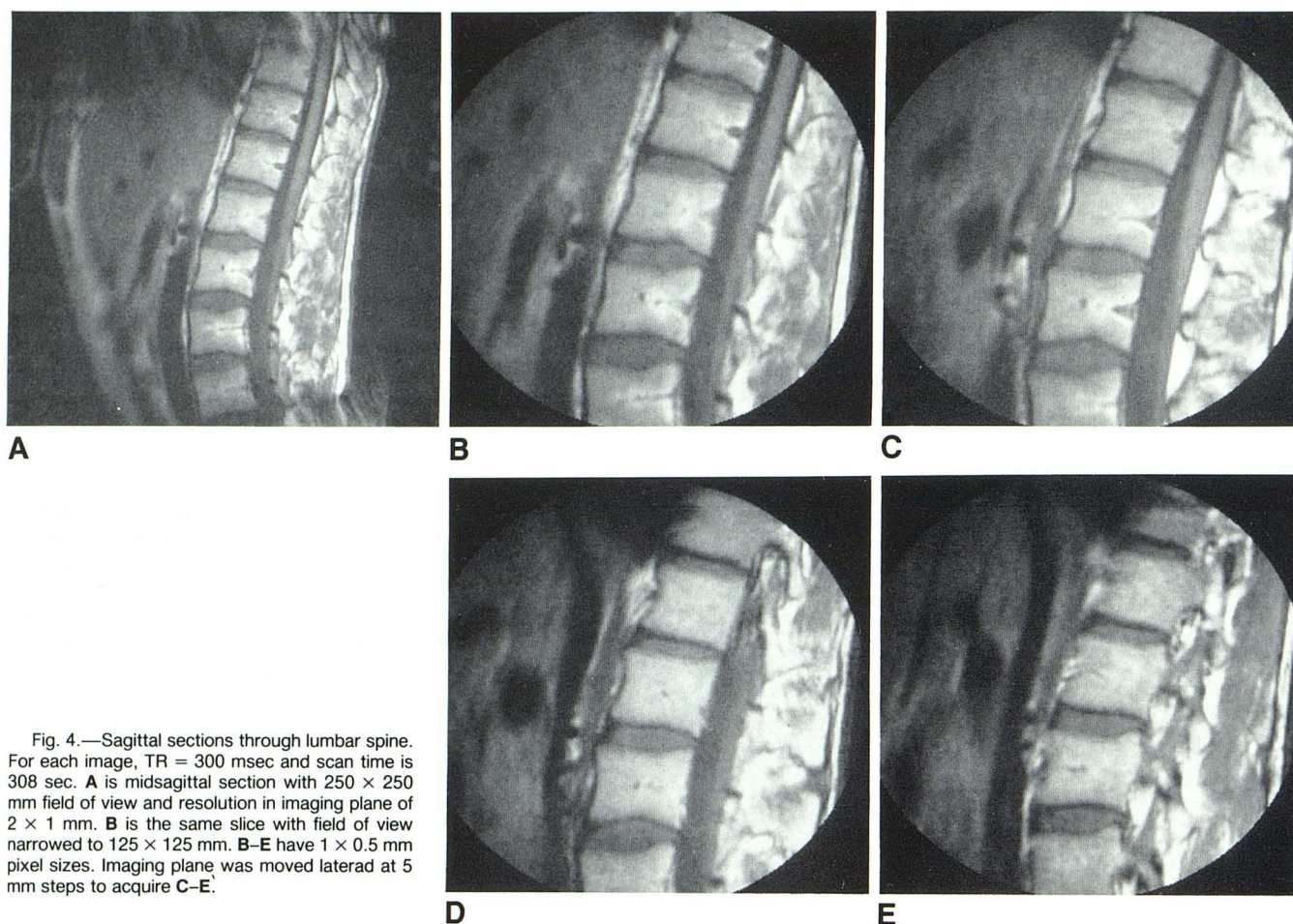
Fig. 4.—Sagittal sections through lumbar spine. For each image, TR = 300 msec and scan time is 308 sec. **A** is midsagittal section with 250 × 250 mm field of view and resolution in imaging plane of 2 × 1 mm. **B** is the same slice with field of view narrowed to 125 × 125 mm. **B–E** have 1 × 0.5 mm pixel sizes. Imaging plane was moved laterad at 5 mm steps to acquire **C–E**.

6. Axel L. Surface coil magnetic resonance imaging. *J Comput Assist Tomogr* **1984**;8:381–384

7. Edelstein WA, Schenck JF, Hart HR, Hardy CJ, Foster TH, Bottomley PA. High resolution NMR imaging at 1.5 Tesla using surface coils. *JAMA* (in press)

8. Edelstein WA, Bottomley PA, Hart HR, Smith LS. Signal, noise and contrast in nuclear magnetic resonance (NMR) imaging. *J Comput Assist Tomogr* **1983**;7:391–401

9. Daniels DL, Pech P, Haughton VM. *Magnetic resonance imaging of the temporal bone.* Milwaukee: General Electric, **1984**

10. Bottomley PA, Hart HR, Edelstein WA, et al. Anatomy and metabolism of the normal human brain studied by magnetic resonance at 1.5 Tesla. *Radiology* **1984**;150:441–446

11. Bottomley PA, Foster TH, Leue WM. Chemical imaging of the brain by NMR. *Lancet* **1984**;1:1120